



01 Jan 2003

Bubble Dynamics Measurements using Four-Point Optical Probe

Junli Xue

Muthanna H. Al-Dahhan

Missouri University of Science and Technology, aldahhanm@mst.edu

M. P. Dudukovic

R. F. Mudde

Follow this and additional works at: https://scholarsmine.mst.edu/che_bioeng_facwork



Part of the [Biochemical and Biomolecular Engineering Commons](#)

Recommended Citation

J. Xue et al., "Bubble Dynamics Measurements using Four-Point Optical Probe," *Canadian Journal of Chemical Engineering*, vol. 81, no. 3 thru 4, pp. 375 - 381, Wiley, Jan 2003.

The definitive version is available at <https://doi.org/10.1002/cjce.5450810306>

This Article - Conference proceedings is brought to you for free and open access by Scholars' Mine. It has been accepted for inclusion in Chemical and Biochemical Engineering Faculty Research & Creative Works by an authorized administrator of Scholars' Mine. This work is protected by U. S. Copyright Law. Unauthorized use including reproduction for redistribution requires the permission of the copyright holder. For more information, please contact scholarsmine@mst.edu.

Bubble Dynamics Measurements Using Four-Point Optical Probe

Junli Xue^{1*}, Muthanna Al-Dahhan¹, M. P. Dudukovic¹ and R. F. Mudde²

¹ Chemical Reaction Engineering Laboratory (CREL), Washington University, St. Louis, MO, USA.

² Kramers Laboratorium voor Fysische Technologie, Delft University of Technology, Delft, The Netherlands

Bubble column reactors are used extensively to perform a wide variety of gas-liquid or gas-liquid-solid reactions such as oxidation, hydrogenation, chlorination, aerobic fermentation, waste water treatment, coal liquefaction, etc. The main advantages of bubble columns compared to other multiphase reactors (stirred vessels, packed beds, etc.) include simple construction, low maintenance due to the absence of moving parts, excellent heat transfer properties, easy temperature control, reasonable interphase mass transfer rates at low energy input, etc.

Bubble dynamics, which include bubble velocity, bubble size, gas hold-up and specific interfacial area, are of considerable importance for the proper design and operation of bubble columns. However, the measurement of bubble size, bubble velocity and specific interfacial area in two and three-phase systems has always been a challenging problem. The problem becomes even more complex when the system is no longer in the bubbly flow regime, but rather in the chaotic churn-turbulent flow regime, which is of predominant industrial interest.

The appeal of non-invasive techniques has led to attempts to capture the bubble size distribution and bubble velocity distribution by video imaging techniques (Marques et al., 1999; Mihai and Pincovski, 1998; Idogawa, 1997; Luewisutthichat et al., 1997). However, video imaging can only be used in two-dimensional transparent columns at low gas holdup, where light can penetrate the system. In real three-dimensional columns, even if they have transparent walls, this technique provides no hope of capturing anything beyond the reactor wall. Video imaging also cannot be used in systems where the columns are operated at high temperature and high pressure and thus cannot be made of transparent materials. Thus, invasive techniques are still the state-of-the-art when it comes to bubble size and bubble velocity measurements in practical three-dimensional multiphase systems.

The microprobes (optical and conductivity probes) have been most frequently employed to investigate the bubble dynamics in recent years (Burgess and Calderbank, 1975; Saxena et al., 1990; Chabot et al., 1992; A. Cartellier, 1998; Luo et al., 1998; Mudde and Saito, 2001). Of the microprobes, the conductivity probes utilize the difference in electrical conductivity between the liquid phase and the gas phase. The optical fiber probes make use of the difference in the refractive index between the gas phase and the liquid phase and provide a sequence of voltage pulses when a bubble passes by the probe. In comparison with conductivity probes, the optical probes offer several advantages: they can be used in

By conducting an analysis of the measurement errors it was found that bubble dynamics obtained by two-point probes can be highly inaccurate. A four-point optical probe with appropriate data processing algorithm has been developed so that the bubble velocity vector can be obtained. This probe provides directly the value of specific gas-liquid interfacial area. However, for obtaining accurate values of bubble velocity and size, the four-point probe must be calibrated by a CCD camera at the same conditions. Calibration columns have been developed for this purpose where the bubble size and velocity can be varied to calibrate the measurements by the four-point optical probe against a CCD camera.

En effectuant une analyse des erreurs de mesure, on a trouvé que la dynamique des bulles obtenue au moyen de sondes à deux points peut être très imprécise. On a donc mis au point une sonde optique à quatre points avec un algorithme de traitement des données approprié de façon à obtenir le vecteur de vitesse des bulles. Cette sonde donne directement la valeur de la région interfaciale gaz-liquide spécifique. Cependant, pour obtenir des valeurs précises de la vitesse et de la taille des bulles, la sonde à quatre points doit être calibrée au moyen d'une caméra CCD avec les mêmes conditions. Des colonnes de calibration ont été mises au point à cette fin là, qui permettent de faire varier la taille et la vitesse des bulles pour calibrer les mesures de la sonde optique à quatre points par rapport à la caméra CCD.

Keywords: bubble column, bubble measurements, four-point optical probe.

conductive as well as in non-conductive (organic) systems; they have better signal/noise ratio; the presence of a liquid film on the sensor tip reduces the effectiveness of a conductivity probe but not that of an optical probe and the sensitivity of optical probes is therefore higher than that of conductivity probes (van der Lans, 1985).

Most researchers have employed two-point probes to measure the bubble dynamics in multiphase systems. However, we show here that bubble

*Author to whom correspondence may be addressed. E-mail address: jlxue@che.wustl.edu

dynamics obtained by two-point probes are not reliable. Hence, a four-point probe was suggested to improve the measurements (Burgess and Calderbank, 1975; Mudde and Saito, 2001). The objective of this paper is to present a four-point optical probe with an improved algorithm for the determination of bubble size and velocity. With this new probe, bubble dynamics can be measured with better accuracy.

The Limitation Of Two-Point Probes

Two-point probes are employed by many researchers to measure bubble velocity and bubble size (Choi and Lee, 1990; Chabot et al., 1992; Wu and Ishii, 1999; Fan et al., 1999; Magaud et al., 2001). Lim and Agarwal (1992) analyzed the errors in the measurements of bubble dynamics by two-point probes based on the assumption of spherical bubbles. They concluded that the measurements obtained by a dual-element probe are theoretically questionable and experimental results reported using these probes must be viewed at best as qualitative. Since more bubbles in bubble columns are approximately ellipsoidal, the case of ellipsoidal bubbles is analyzed in this paper. It is found again that the measurements of the bubble velocity and bubble size by two-point probes can be highly inaccurate.

To analyze the measurement errors in the bubble velocity and bubble chord length obtained by a two-point probe, some assumptions are made (refer to Figure 1):

- 1) The bubbles have a symmetry plane (e.g. spherical or ellipsoidal bubbles) that is perpendicular to the bubble velocity vector.
- 2) The bubble shape fluctuation and deformation of the bubble due to its interaction with the probe are neglected.
- 3) The bubble velocity vector (magnitude and direction) does not change during the bubble passage by the probe.

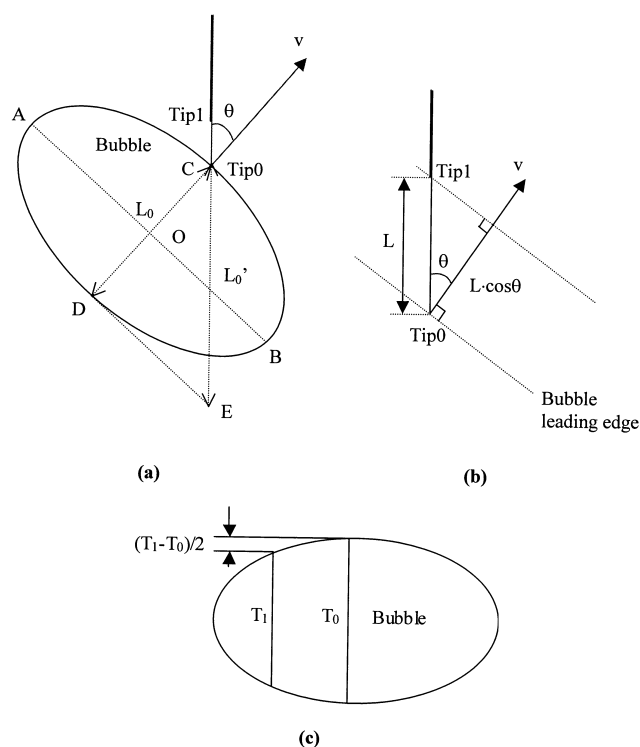


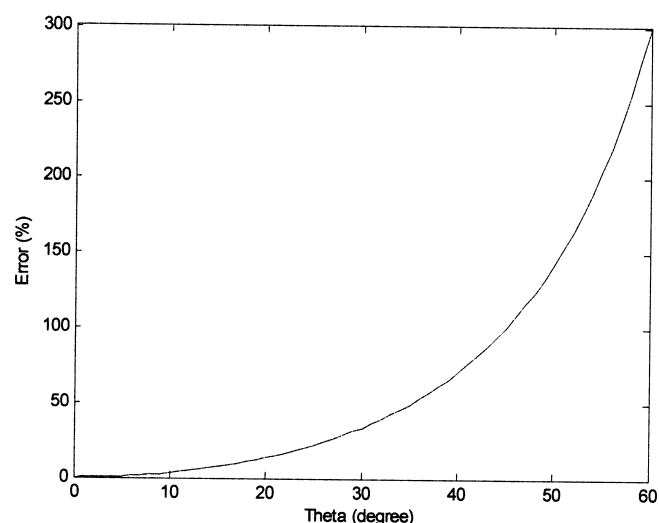
Figure 1. Schematic of the bubble measurement by a two-point probe.

With these assumptions, the time interval between the time instance when the leading edge of a bubble hits Tip0, the longer tip of a two-point probe (Figure 1a), and that when it hits Tip1, the shorter tip of a two-point probe, Δt , is (refer to Figure 1b):

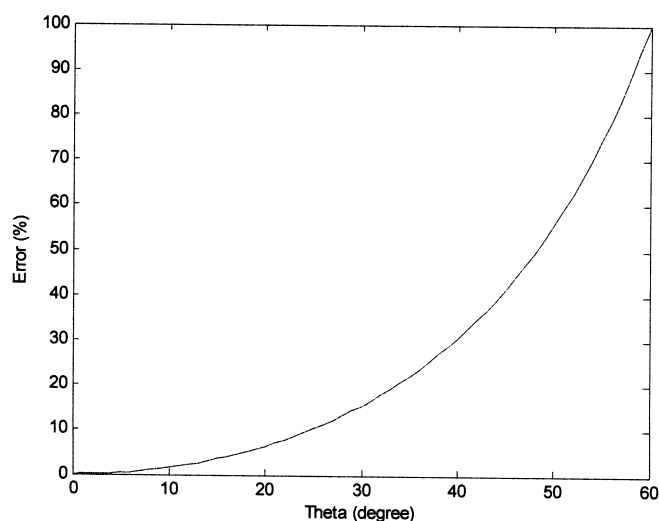
$$\Delta t = \frac{L \cdot \cos \theta}{v} \quad (1)$$

where v is the magnitude of the bubble velocity vector; θ is the angle between the bubble velocity vector and the probe axial direction (Figure 1a).

A closer examination reveals that Equation (1) is not accurate because the curvature of the bubble's leading edge is



(a)



(b)

Figure 2. Relative error in (a) the bubble vertical velocity and (b) the bubble chord length obtained by a two-point probe.

neglected. In fact, the effect of curvature on the measurements by two-point probes was neglected in most of the published studies (Choi and Lee, 1990; Chabot et al., 1992; Wu and Ishii, 1999; Fan et al., 1999; Magaud et al., 2001). To obtain the velocity of a bubble, the displacement of the bubble's centroid instead of that of the bubble's leading edge needs to be known. The centroid of an ellipsoidal bubble (or any bubble that is symmetric to the major plane of the bubble) is on the plane formed by the major axes of the bubble, i.e. plane AOB in Figure 1a. Hence, Equation (1) is adjusted to account for the bubble's curvature as follows (refer to Figure 1c):

$$\Delta t - \frac{T_1 - T_0}{2} = \frac{L \cos \theta}{v} \quad (2)$$

where T_0 and T_1 are the time intervals that Tip0 and Tip1 spend in the bubble, respectively.

The magnitude of the vertical component of the bubble velocity vector with an angle θ to the vertical direction is then customarily obtained as (Korekazu et al., 1980; Lim and Agarwal, 1992; Choi and Lee, 1990):

$$v_z' = \frac{L}{\Delta t - \frac{T_1 - T_0}{2}} = \frac{v}{\cos \theta} \quad (3)$$

However, the real magnitude of the vertical component of the bubble velocity vector is (see Figure 1b):

$$v_z = v \cos \theta \quad (4)$$

The relative error in the measurements of the bubble vertical velocity component is:

$$\text{Error} = \frac{v_z' - v_z}{v_z} \times 100\% = (\tan \theta)^2 \times 100\% \quad (5)$$

The relative errors predicted by Equation (5) are shown in Figure 2a. It can be seen that the errors are always nonnegative, i.e. the magnitude of the bubble velocity vector obtained by two-point probes is always larger than the real value; the errors increase with the value of θ ; it can be as large as 100% at $\theta = 45^\circ$, and it is even larger at larger θ values until it goes to infinity at $\theta = 90^\circ$.

Since the bubble chord length is obtained by the product of the bubble vertical velocity and the time interval that the probe tip spends in the bubble, the error in the bubble velocity is

transferred to the bubble chord length. The equation to obtain the chord length pierced by Tip0 is:

$$L_0' = v_z' T_0 = \frac{v}{\cos \theta} \cdot \frac{L_0}{v} = \frac{L_0}{\cos \theta} \quad (6)$$

where L_0 is the real chord length pierced by Tip0 and L_0' is the bubble chord length obtained by a two-point probe. Actually, $L_0/\cos \theta$ represents the length CE in Figure 1a, while the real chord length pierced by Tip0, L_0 , is that of CD.

The relative error in the bubble chord length pierced by Tip0 is:

$$\text{Error} = \frac{L_0' - L_0}{L_0} \times 100\% = \left(\frac{1}{\cos \theta} - 1 \right) \times 100\% \quad (7)$$

As shown in Figure 2b, this error is also always positive, i.e. the bubble chord length obtained by two-point probes is always larger than the real chord length pierced by the probe tip; the error increases with the value of angle θ , and it can be as great as 40% at $\theta = 45^\circ$.

The above analysis indicates that measurements of bubble dynamics by two-point probes are subject to large errors. Reasonably accurate measurements are possible only for very small angles θ , i.e. for small departure of the bubble velocity vector from the line that connects the two tips of the two-point probe. Hence, two-point probes can only be used in the situations where all bubbles move strictly in one direction, such as in forced cocurrent gas liquid flow in pipes, and are not suitable for systems having complex flow dynamics as bubble columns. New probes and algorithms need to be designed to obtain these important parameters in bubble column flows.

The Four-Point Optical Probe And The Proposed Data Processing Algorithm

Frijlink (1987) and his colleagues at the University of Delft in the Netherlands employed a four-point optical probe (Figure 3) to measure the bubble velocity and bubble size in bubble columns. Three of the four tips of the probe are of the same length and form an equilateral triangle. The fourth central tip is positioned through the inertial centre of this triangle and is about 2.0mm longer than the others. The radial distance from the central fiber to each of the others that surround it is about 0.6mm. Theoretically, this four-point probe can distinguish those bubbles moving in the probe's axial direction ($\theta = 0^\circ$) and hence, measure only the velocity and chord lengths of these bubbles. From Figures 2, it can be seen that, theoretically, the relative errors in the bubble velocity and bubble chord lengths go to zero at $\theta = 0^\circ$. However, in bubble columns, bubbles that strictly move in the probe's axial direction are only a small part of the whole population of bubbles. For example, in a two-dimensional column, we found that about 99% of bubbles that hit the four-point optical probe were discarded due to the deviation of the bubble velocity from the probe's axial direction. This would make the bubble velocity and size distributions obtained by the four-point optical probe questionable because there is neither theoretical nor experimental proof that the velocity and size distribution of the whole bubble population can be represented by that of a specific part of the bubbles.

The four-point probe shown in Figure 3 was constructed and employed in our research while a new algorithm for data

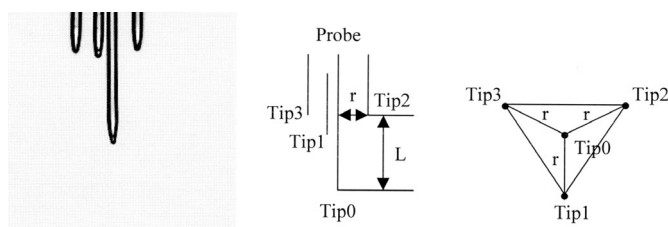


Figure 3. Schematic of the four-point optical probe.

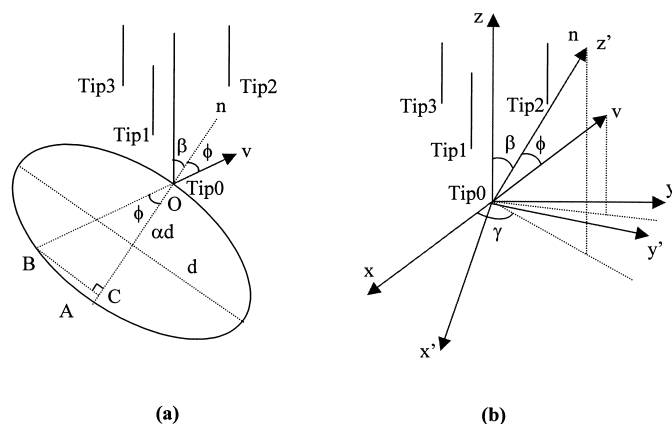


Figure 4. Schematic of the bubble measurements by the four-point optical probe.

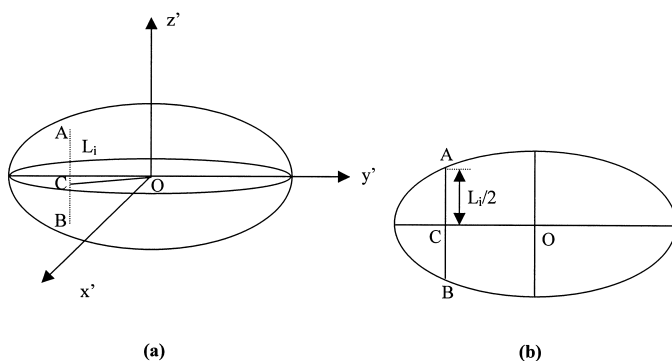


Figure 5. Determination of bubble size and aspect ratio by the four-point optical probe.

processing has been developed to increase the capability of the probe and accuracy of its measurements. With this new data processing algorithm, there is no need for selecting only a specific population of bubbles (e.g. bubbles moving in the probe's axial direction) and hence, the whole bubble population can be used to determine the characteristics of the bubble dynamics.

Figure 4a shows the schematic when a bubble hits the four-point optical probe. From Figure 4c, assuming the bubbles are ellipsoidal (this assumption is valid only in the case of bubbly flow) and considering the surface curvature of the bubbles, it can be derived that the time intervals between the time when a bubble hits the central tip Tip0 and that when it hits Tip i , $i = 1, 2, 3$ are:

$$\Delta t_1 - \frac{T_1 - T_0}{2} = \frac{z'_1 / \cos \phi}{v} = \frac{x_1 \sin \beta \cos \gamma + y_1 \sin \beta \sin \gamma + z_1 \cos \beta}{v \cos \phi} \quad (8a)$$

$$\Delta t_2 - \frac{T_2 - T_0}{2} = \frac{z'_2 / \cos \phi}{v} = \frac{x_2 \sin \beta \cos \gamma + y_2 \sin \beta \sin \gamma + z_2 \cos \beta}{v \cos \phi} \quad (8b)$$

$$\Delta t_3 - \frac{T_3 - T_0}{2} = \frac{z'_3 / \cos \phi}{v} = \frac{x_3 \sin \beta \cos \gamma + y_3 \sin \beta \sin \gamma + z_3 \cos \beta}{v \cos \phi} \quad (8c)$$

where v is the magnitude of the bubble velocity vector, β is the angle between the normal vector (vector n in Figure 4b) of the bubble's symmetry plane to the probe's axial direction (z direction), γ is the angle between the projection of the normal vector on the xy plane to the x axis (Figure 4b), ϕ is the angle between the bubble velocity vector and the normal vector of the symmetry plane of the bubble. The values of $x_i, y_i, z_i, i = 1, 2, 3$, are the coordinates of Tip 1, 2, 3 of the probe, obtained photographically. $T_i, i = 0, 1, 2, 3$ is the time interval that Tip i spends in the bubble.

After calculating the bubble velocity by solving Equations (8a), (8b) and (8c), the bubble dimension can be obtained by solving the following equations (refer to Figure 5):

$$\left(\frac{L_0}{2}\right)^2 + \alpha^2[(x'_0 - O_{x'})^2 + (y'_0 - O_{y'})^2] = \alpha^2 d^2 \quad (9a)$$

$$\left(\frac{L_1}{2}\right)^2 + \alpha^2[(x'_1 - O_{x'})^2 + (y'_1 - O_{y'})^2] = \alpha^2 d^2 \quad (9b)$$

$$\left(\frac{L_2}{2}\right)^2 + \alpha^2[(x'_2 - O_{x'})^2 + (y'_2 - O_{y'})^2] = \alpha^2 d^2 \quad (9c)$$

$$\left(\frac{L_3}{2}\right)^2 + \alpha^2[(x'_3 - O_{x'})^2 + (y'_3 - O_{y'})^2] = \alpha^2 d^2 \quad (9d)$$

where L_i is the bubble chord length pierced by Tip $i, L_i = vT_i$, α is the aspect ratio of a ellipsoidal bubble, $\alpha = (\text{length of vertical axis})/(\text{length of horizontal axis})$, d is the length of the bubble's major axis, $O_{x'}$ and $O_{y'}$ are the x' and y' coordinates of the bubble's center O in the $x'y'z'$ coordinate system (refer to Figure 4b), $x'_i, y'_i, i = 0, 1, 2, 3$, are the coordinates of Tip i in the $x'y'z'$ coordinate system:

$$\begin{aligned} x'_i &= (1 - (1 - \cos \theta) \cos^2 \phi) x_i - (1 - \cos \theta) \sin \phi \cos \phi y_i - \sin \theta \cos \phi z_i \\ y'_i &= -(1 - \cos \theta) \sin \phi \cos \phi x_i + (1 - (1 - \cos \theta) \sin^2 \phi) y_i - \sin \theta \sin \phi z_i \end{aligned} \quad (10)$$

Equations (8a), (8b) and (8c) form a group of nonlinear equations that do not yield analytical solutions. They need to be solved numerically. Since there are only three equations (Equations 8a, 8b, 8c) for four variables, i.e. v, β, γ and ϕ , one can obtain only β, γ and $v \cos \phi$, i.e. v and ϕ cannot be obtained separately. The chord length obtained by the probe is $vT_i \cos \phi$, e.g. in the case of Figure 4a, the chord length pierced by Tip0 is OA but $vT_0 \cos \phi$ is actually the length of OC . Hence, in the case when the bubble velocity vector is not perpendicular to the bubble's symmetry plane ($\phi \neq 0^\circ$), even the four-point probe cannot determine the bubble velocity vector and bubble chord length precisely.

However, Lim and Agarwal (1992) found that in a two-dimensional fluidized bed, ϕ has a normal distribution with the mean of zero and standard deviation of 14° . Kataoka et al. (1986) adopted an upper limit of 10° to 22° for ϕ under different operating conditions in air-water bubbly and slug flow in a vertical tube of inner diameter of 6 cm. Hence, it is reasonable to assume that in most cases the value of ϕ is less than 30° in bubbly flow. At $\phi = 30^\circ$, $\cos \phi = 0.866$. This means at $\phi = 30^\circ$, $v \cos \phi$ is 13.4% smaller than v . At ϕ less than 30° , the error will be less than 13.4%. Therefore, if we accept the value of $v \cos \phi$ obtained by the probe as the bubble velocity, the estimated values will be less than real values within 13%. Hence, Equations (8) and (9) would be applied to determine the

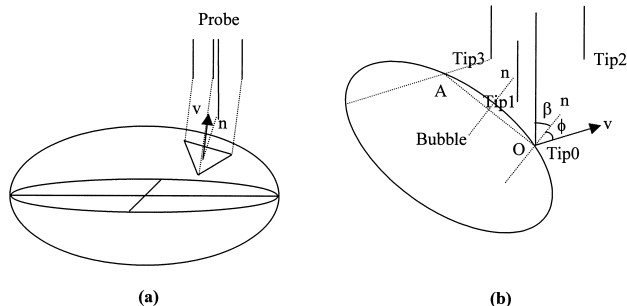


Figure 6. Specific interfacial area measurement by the four-point optical probe.

bubble velocity distribution and bubble size distribution with engineering accuracy in bubbly flow with the bounding error mentioned above. Note that in the analysis of the errors in the measurements by two-point probes, we assumed that the bubble velocity vector aligns the normal vector of the symmetry plane of the bubble (bubble orientation), i.e. $\phi = 0^\circ$. When ϕ is not equal to 0° , it will cause additional errors in the bubble velocity and bubble chord length obtained by two-point probes.

Kataoka et al. (1986) derived the Equation for the local specific interfacial area, a , in gas-liquid systems as:

$$a = \frac{N}{\Delta T} \frac{1}{\overline{v \cos \phi}} = \frac{1}{\Delta T} \sum \frac{1}{v \cos \phi} \quad (11)$$

where N is the total number of the gas-liquid interfaces passing by the probe during the measurement time Δt , ϕ is the angle between the velocity vector and the normal vector of the interface (bubble's surface). These researchers employed two-point and four-point probes to determine the interfacial area based on Equation (11) (Revankar and Ishii, 1993; Wu and Ishii, 1999). However, in their measurements, the assumption about the bubble's shape was needed so that the measurement can only be applied in bubbly flow since, in churn-turbulent flow, many bubbles are of irregular shape.

The four-point optical probe, together with the proposed data processing algorithm developed in this study, can be employed to obtain the local specific interfacial area both in bubbly flow and in churn-turbulent flow based on Equation (11). To measure the specific interfacial area by two-point probes, many more assumptions about the bubble shape and movement are needed (Wu and Ishii, 1999). The schematic of the measurements is shown in Figure 6. Assume that the section of the gas-liquid interface (bubble surface) between the three tips, Tip1, Tip2 and Tip3, of the probe (refer to Figure 6a) is flat.

The equation for determining the velocity of the section of bubble's surface are:

$$\begin{aligned} \Delta t_1 &= \frac{z'_1 / \cos \phi}{v} = \frac{x_1 \cdot \sin \beta \cos \gamma + y_1 \cdot \sin \beta \sin \gamma + z_1 \cdot \cos \beta}{v \cdot \cos \phi} \\ \Delta t_2 &= \frac{z'_2 / \cos \phi}{v} = \frac{x_2 \cdot \sin \beta \cos \gamma + y_2 \cdot \sin \beta \sin \gamma + z_2 \cdot \cos \beta}{v \cdot \cos \phi} \quad (12a) \\ \Delta t_3 &= \frac{z'_3 / \cos \phi}{v} = \frac{x_3 \cdot \sin \beta \cos \gamma + y_3 \cdot \sin \beta \sin \gamma + z_3 \cdot \cos \beta}{v \cdot \cos \phi} \end{aligned}$$

By solving these three equations numerically, the value of $v \cdot \cos \phi$ is obtained, which can then be used to obtain the specific interfacial area from Equation (11). However, if a bubble hit the central tip of the probe but misses some other tips, then the bubble surfaces' velocity vector cannot be obtained by solving Equations (12a), (12b) and (12c). To account for the contribution of these missed bubbles to the specific interfacial area, the average value of $v \cdot \cos \phi$ of the bubbles measured is assigned to these missed bubbles.

$$a = \frac{1}{\Delta T} \cdot \sum \frac{1}{v \cdot \cos \phi} \cong \frac{1}{\Delta T} \cdot \frac{N}{N_{measured}} \sum \frac{1}{v \cdot \cos \phi} \quad (13a)$$

$$N = N_{measured} + N_{missed} \quad (13b)$$

Equations (12) and (13) do not need the assumption about the bubble shape. Hence, they are valid both in bubbly flow and in churn-turbulent flow. As a result, the specific interfacial area both in bubbly flow and in churn-turbulent flow can be obtained by the measurements of the four-point optical probe.

The Calibration of the Probe

It was found in this research that the magnitude of the bubble velocity vector obtained by the probe is always smaller than the real value. One of the possible reasons is that when bubbles hit the probe tip, the interaction between the probe and the bubble dents the bubble's leading edge. This also affects the measurements of bubble chord length. Hence, the calibration of the probe needs to be accomplished before the probe can be applied in practical bubble columns to ensure that the measurements of bubble velocity and bubble chord length by the four-point probe are reliable. The probe calibration is accomplished by comparing the bubble velocity and bubble chord length obtained by the probe with those obtained by a CCD camera. Figure 7 shows the experimental set up for the calibration. The set-up calibration column consists of an outer pipe and an inner pipe (both are square to avoid image distortion caused by the curvature of circular pipe wall).

By adjusting the valve on the liquid flow circuit, the liquid flow rate in the inner pipe can be controlled. Since the bubble rises with the liquid, the velocity of the bubble can be adjusted to different desired values.

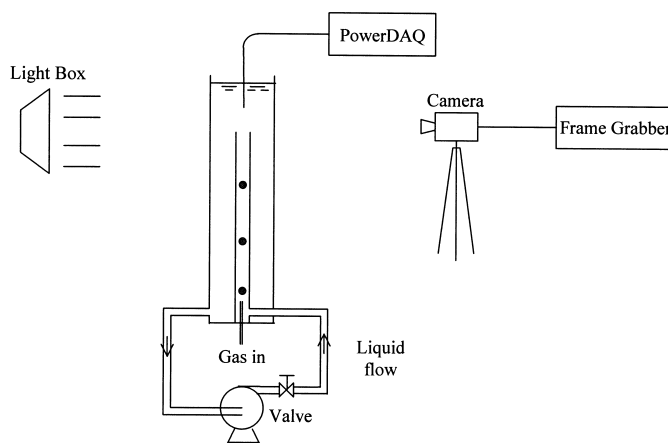


Figure 7. Schematic of the probe calibration set-up.

By calibration, correction factors for both the bubble velocity and the bubble chord length obtained by the probe will be determined (Equation (14)). The correction factor is the ratio of the bubble velocity or bubble chord length obtained by the camera to those obtained by the four-point probe. The bubble velocity and bubble chord length obtained by the probe can be corrected by multiplying the measured values with correction factors:

$$v = v' \text{ correction factor}$$

$$L_i = L'_i \text{ correction factor} \quad (14)$$

$$\text{correction factor} = \frac{\text{Values obtained by camera}}{\text{Values obtained by probe}} = f(v', d')$$

In Equation (14) v is the magnitude of the bubble velocity, v' is the magnitude of the bubble velocity obtained by the probe, d' is the length of the bubble's major axis obtained by the probe, L_i is the bubble chord length pierced by the probe Tip i , L'_i is the bubble chord length obtained by the probe.

Preliminary probe calibration results show that the correction factor for the bubble velocity obtained by the probe did not change much with bubble size in the range of 0.3 cm to 1.8 cm of volume-equivalent bubble diameter and with bubble velocity in the range of 28.1 cm/s to 58.5 cm/s. The average is 1.13. Theoretically, the calibration factors depend on the physical properties (viscosity, surface tension etc.) of the liquid system, i.e. the calibration factors will be different for different liquid systems. Hence, if the probe will be used in a new liquid system, calibration in this liquid system against the camera is needed. The calibration factors for the probes of the same configuration stay the same in the experiments, since the probes are made of the same materials and they are similar in configuration to each other. Hence, calibration for new a probe of the same configuration is unnecessary.

The complete results of the probe calibration, the verification of the specific interfacial area obtained by the probe with the camera, and the application of the probe in bubble columns will be presented in following papers.

Summary and Conclusions

The results of numerical simulation showed that bubble velocity and bubble size obtained by two-point probes are not reliable. The errors can be very large. Hence, a four-point optical probe was employed to investigate the bubble dynamics in a multiphase system. A new data processing algorithm was developed. With this new algorithm, not only the bubble velocity and bubble size, but also the specific interfacial area can be measured. While specific interfacial area determination does not require calibration, for bubble velocity and chord length measurements in bubble columns the probe needs to be calibrated against a CCD camera in a calibration column.

Acknowledgements

Partial support from DOE Contract FC 2295 PC 95051 via Air Products is gratefully acknowledged. The authors are also grateful to B.A. Toseland of Air Products for many fruitful discussions.

Nomenclature

a	specific interfacial area, (mm ² /mm ³)
d	the length of the bubble's major axis, (mm)

L_i	the bubble chord length pierced by Tip i , (mm)
N	the total number of the gas-liquid interfaces passing by the probe during the measurement time
$O_{x'}, O_{y'}$	the x' and y' coordinates of the bubble's center O in the $x'y'z'$ coordinate system, (mm)
Δt_i	time intervals between a bubble hitting the central tip T_0 and it hitting tip T_i (s)
Δt	measurement time, (s)
$T_i, i = 0, 1, 2, 3$	the time interval that Tip i spend in the bubble, (s)
v	the magnitude of the bubble velocity vector, (mm/s)
v'	the magnitude of the bubble velocity vector obtained by the probe, (mm/s)
v_z	the magnitude of the vertical component of the bubble velocity vector, (mm/s)
v'_z	the magnitude of the vertical component of the bubble velocity vector obtained by the probe, (mm/s)
$x_p, y_p, z_p, i = 1, 2, 3$	the coordinates of Tip 1, 2, 3 of the probe, (mm)
$x'_i, y'_i, i = 0, 1, 2, 3$	the coordinates of Tip i in the $x'y'z'$ coordinate system, (mm)

Greek Symbols

α	the aspect ratio of the bubble, $\alpha = (\text{length of minoraxis})/(\text{length of major axis})$
β	the angle between the normal vector of the bubble's symmetry plane to the probe's axial direction
γ	the angle between the projection of the normal vector on the xy plane to the axis x
θ	the angle of the bubble velocity vector to the probe's axial direction
ϕ	the angle between the bubble velocity vector and the normal vector of the symmetry plane of the bubble

References

- Burgess J.M. and P.H. Calderbank, "The Measurement Of Bubble Parameters In Two-Phase Dispersions I: The Development Of An Improved Probe Technique", Chem. Eng. Sci. **30**, 743–750 (1975).
- Cartellier, A., "Measurement Of Gas Phase Characteristics Using New Mono-optical Fiber Probes And Real Time Signal Processing", Nucl. Eng. Des. **184**, 393–408 (1998).
- Chabot, J., S.L.P. Lee, A. Soria and H.I. de Lasa, "Interaction Between Bubbles And Fiber Optic Probes In A Bubble Column", Can. J. Chem. Eng. **70**, 61–68 (1992).
- Choi, K.H. and W.K. Lee, "Comparison Of Probe Methods For Measurement Of Bubble Properties", Chem. Eng. Comm. **91**, 35–47 (1990).
- Fan L-S., G.Q. Yang, D.J. Lee, K. Tsuchiya and X. Luo, "Some Aspects Of High-Pressure Phenomena Of Bubbles In Liquids And Liquid-Solid Suspensions", Chem. Eng. Sci. **54**, 4681–4709 (1999).
- Frijlink, J.J., "Physical Aspects Of Gassed Suspension Reactors", Ph. D. Thesis, Delft University of Technology, Delft, The Netherlands (1987).
- Idogawa, K., "Methods For Measurement Of Gas Hold-Up And Gas Bubble Diameter In A High-Pressure Bubble Column", Kagaku Kagaku **61**, 781–782 (1997).
- Kataoka, I., M. Ishii and A. Serizawa, "Local Equationtion And Measurements Of Interfacial Area Concentration In Two-Phase Flow", Int. J. Multiphase Flow **12**, 505–529 (1986).
- van der Lans, R.G.J.M., dissertation, Delft University of Technology, Delft, The Netherlands (1985).
- Lim, K.S. and P.K. Agarwal, "Bubble Velocity In Fluidized Beds: The Effect Of Non-Vertical Bubble Rise On Its Measurement Using

- Submersible Probes And Its Relationship With Bubble Size", *Powder Tech.* **69**, 239–248 (1992).
- Luewisutthichat, W., A. Tsutsumi and K. Yoshida, "Bubble Characteristics In Multi-Phase Flow Systems: Bubble Sizes And Size Distribution", *J. Chem. Eng. Jpn.* **30**, 461–466 (1997).
- Luo, X., G. Yang, D.J. Lee and L-S. Fan, "Single Bubble Formation In High Pressure Liquid–Solid Suspensions", *Powder Tech.* **100**, 103–112 (1998).
- Marques, J.J.P. and R. Bouard, "Bubbles In A Gas–Solid Fluidized Bed. Photographic Characterization", *Tech. Mod.* **91**, 20–24 (1999).
- Mihai, M. and I. Pincovski, "Experimental Study Of Bubble Size Distribution In A Bubble Column", *Sci. Technol. Environ. Prot.* **5**, 34–41 (1998).
- Mudde R.F. and T. Saito, "Hydrodynamical Similarities Between Bubble Column And Bubbly Pipe Flow", *J. Fluid Mech.* **437**, 203–228 (2001).
- Revankar S.T. and M. Ishii, "Theory And Measurement Of Local Interfacial Area Using A Four Sensor Probe In Two-Phase Flow", *Int. J. Heat Mass Transfer* **36**, 2997–3007 (1993).
- Saxena, A.C., N.S. Rao and S.C. Saxena, "Bubble Size Distribution In Bubble Columns", *Can. J. Chem. Eng.* **68**, 159–161 (1990).
- Wu, Q. and M. Ishii, "Sensitivity Study On Double-Sensor Conductivity Probe For The Measurement Of Interfacial Area Concentration In Bubbly Flow", *Int. J. Multi. Flow* **25**, 155–173 (1999).
- Magaud, F., M. Souhar, G. Wild and N. Boisson., "Experimental Study Of Bubble Column Hydrodynamics", *Chem. Eng. Sci.* **56**, 4597–4607 (2001).

Manuscript received October 31, 2002; revised manuscript received April 1, 2003; accepted for publication April 7, 2003.